T2R2 東京科学大学 リサーチリポジトリ
Science Tokyo Research Repository

論文 / 著書情報
Article / Book Information

Title	Thermal stability of supersaturated Mg_x_Zn_1-x_O alloy films and Mg_x_Zn_1-x_O/ZnO heterointerfaces
Authors	A. Ohtomo,R. Shiroki,I. Ohkubo,H. Koinuma,M. Kawasaki
Citation	Applied Physics Letters, Vol. 75, No. 26,
Pub. date	1999, 12
URL	http://scitation.aip.org/content/aip/journal/apl
Copyright	Copyright (c) 1999 American Institute of Physics

Powered by T2R2 (Science Tokyo Research Repository)

Thermal stability of supersaturated $Mg_xZn_{1-x}O$ alloy films and $Mg_xZn_{1-x}O$/ZnO heterointerfaces

A. Ohtomo[a] and R. Shiroki
Department of Innovative and Engineered Materials, Tokyo Institute of Technology, Yokohama 226-8502, Japan

I. Ohkubo and H. Koinuma[b]
Materials and Structures Laboratory, Tokyo Institute of Technology, Yokohama 226-8502, Japan

M. Kawasaki[c]
Department of Innovative and Engineered Materials, Tokyo Institute of Technology, Yokohama 226-8502, Japan

(Received 13 August 1999; accepted for publication 29 October 1999)

We have examined the thermal stability of wurtzite-phase $Mg_xZn_{1-x}O$ alloy films and ZnO/$Mg_xZn_{1-x}O$ bilayer films with x exceeding the reported solubility limit of 0.04. When a $Mg_{0.23}Zn_{0.78}O$ film was annealed, the segregation of MgO started at 850 °C and the band gap was reduced to the value of that for an $x=0.15$ film after annealing at 1000 °C. $Mg_{0.15}Zn_{0.85}O$ films showed no change of the band gap even after annealing at 1000 °C. Therefore, we conclude that the thermodynamic solubility limit of MgO in $Mg_xZn_{1-x}O$ epitaxial film is about $x=0.15$. The thermal diffusion of Mg across the $Mg_xZn_{1-x}O$/ZnO interface was observed only after annealing above 700 °C. Unlike other II–VI semiconductors, ZnO-based alloy films and heterointerfaces are stable enough for the fabrication of high-crystallinity heterostructures. © *1999 American Institute of Physics.* [S0003-6951(99)00852-9]

As a possible candidate among wide-gap semiconductor materials for short-wavelength light-emitting devices (LEDs), the oxide semiconductor ZnO is attracting considerable attention. The first ultraviolet laser action in ZnO was reported by Reynolds, Look, and Jogai, but that was from a bulk ZnO single crystal at 2 K.[1] We reported excitonic-stimulated emission for ZnO epitaxial films upon optical pumping even at room temperature.[2] Exciton collision processes dominate the stimulated emission, giving rise to a very low threshold (24 kW/cm^2). This triggered the intensive research of this field, and laser action at room temperature was reported independently by Bagnall *et al.*,[3] and us.[4] In our case, ZnO thin films grown on sapphire(0001) substrates are composed of hexagonally shaped nanocrystals assembled in a honeycomb fashion.[5] Grain boundaries between nanocrystals around the edge of the excitation stripe act as mirrors to form a longitudinal cavity.[6]

Two important requirements for realizing devices based on $p-n$ junctions such as LEDs and laser diodes are valence control of ZnO to produce p-type material, and band-gap engineering. The former is under intensive study both experimentally[7] and theoretically.[8] The latter has been partly fulfilled by the development of alloy semiconductors of $Mg_xZn_{1-x}O$ (Refs. 9 and 10) and $Zn_{1-x}Cd_xO$ (Ref. 11) to span the band-gap region between 3.0 and 4.0 eV at room temperature. ZnO/$Mg_xZn_{1-x}O$ superlattices have been readily prepared to demonstrate quantum size effects.[12] Alloy films having $x>0.04$ in wurtzite-phase (WZ) $Mg_xZn_{1-x}O$, however, should be considered as a metastable phase because the solubility limit in the MgO–ZnO binary system was reported to be 4 mol % of MgO (Ref. 13). Therefore, it is important to know the stability of supersaturated alloy films, and their interfaces with pure ZnO films.

In this study, we have annealed $Mg_xZn_{1-x}O$ films ($x=0.15$, 0.22) and $Mg_xZn_{1-x}O$/ZnO heterostructures ($x=0.15$, 0.23) at various temperatures up to 1000 °C to examine the thermal stability.

The films were grown on sapphire(0001) substrates at a substrate temperature of 550 °C by laser molecular-beam epitaxy (LMBE) from sintered ceramic targets in 1×10^{-6} Torr of oxygen atmosphere. The Mg content of the as-deposited films, determined by inductively coupled plasma emission analysis, was found to be more than that of the targets, as reported previously.[9] The crystalline structure was examined by powder x-ray diffraction (XRD). The transmission spectrum in the ultraviolet–visible region was measured at room temperature to determine the band gap (E_g) by using the relationship $\alpha^2 \propto h\nu - E_g$, where α is the absorption coefficient and $h\nu$ is the photon energy. The films were successively annealed at 400, 550, 700, 850, and 1000 °C for 1 h in 1 atm of oxygen. Transmission spectroscopy, scanning electron microscopy (SEM), and XRD measurements were carried out after each annealing.

Figure 1 shows the XRD patterns for a 150-nm-thick $Mg_{0.22}Zn_{0.78}O$ alloy film. The as-deposited film was a highly crystalline single phase as verified by sharp (0004) doublet peaks due to Cu$K\alpha_1$ and $K\alpha_2$ for c-axis oriented WZ $Mg_xZn_{1-x}O$, with no detectable rocksalt-phase (RS) impurity (MgO). Up to an 850 °C annealing temperature, the impurity phase peak was hardly observed. After the film was annealed at 1000 °C, a small RS(200) peak appeared at 42.82° of 2θ, indicating that the supersaturated film precipi-

[a]Electronic mail: ohtomo@oxide.rlem.titech.ac.jp
[b]Also a member of CREST, Japan Science and Technology Corporation.
[c]Electronic mail: kawasaki@oxide.rlem.titech.ac.jp

 © 1999 American Institute of Physics
Downloaded 27 Oct 2004 to 130.34.226.195. Redistribution subject to AIP license or copyright, see http://apl.aip.org/apl/copyright.jsp

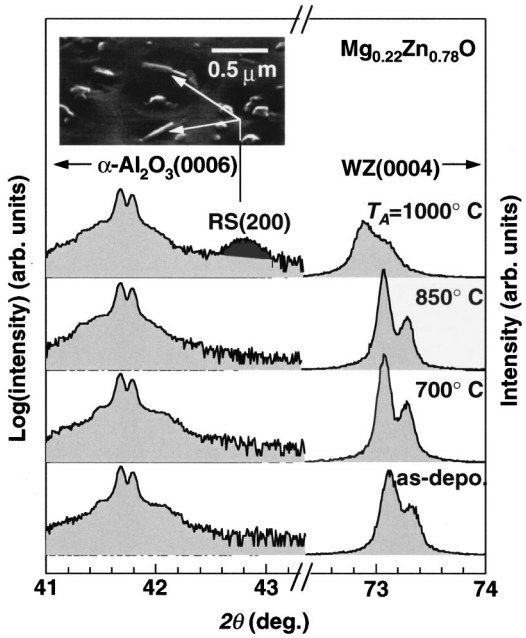


FIG. 1. X-ray diffraction (XRD) pattern for as-deposited $Mg_{0.22}Zn_{0.78}O$ film and those after annealing at $T_A = 700$, 850, and 1000 °C. The left-hand traces containing peaks for the substrate and rocksalt-phase (RS) $Mg_xZn_{1-x}O(200)$ segregation, are plotted on a logarithmic scale, whereas the right-hand traces showing wurtzite-phase (WZ) $Mg_xZn_{1-x}O(0004)$ are plotted on a linear scale. The inset shows a SEM image of the film surface having precipitates after annealing at 1000 °C.

tates RS $Mg_xZn_{1-x}O$ as a secondary phase. The lattice constant of RS $Mg_xZn_{1-x}O$ was calculated to be 4.221 Å, slightly larger than that of pure MgO (4.211 Å). This lattice constant corresponds to that of RS $Mg_{0.46}Zn_{0.54}O$ bulk ceramic.[14] The crystallinity of the WZ $Mg_xZn_{1-x}O$ matrix was considerably degraded due to the segregation. A SEM image of the film annealed at 1000 °C shows rectangular-shaped precipitates of about 400 nm×50 nm size, as shown in the inset of Fig. 1. Much smaller (100 nm×40 nm) precipitates could be seen in the SEM image for the film annealed at 850 °C, indicating the initiation of segregation. For a 150-nm-thick $Mg_{0.15}Zn_{0.85}O$ film, successive annealing up to 1000 °C did not result in any segregation of RS impurity.

The E_g values for the annealed films are plotted in Fig. 2. For the $x = 0.15$ film, the E_g value stayed constant at about

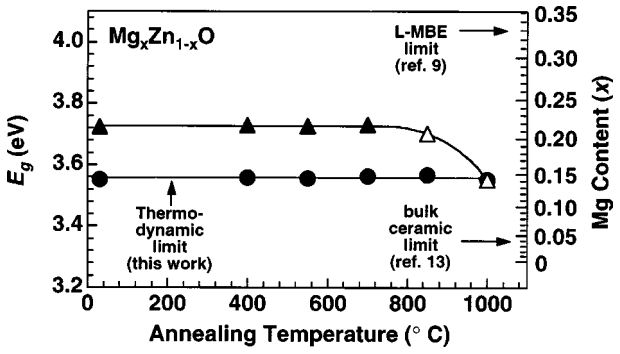


FIG. 2. Band gap (E_g) of $Mg_{0.15}Zn_{0.85}O$ (●) and $Mg_{0.22}Zn_{0.78}O$ (▲ and △) films after annealing for 1 h at temperatures given on the horizontal axis. Open triangles correspond to the samples having a rocksalt phase as precipitates. The thermodynamic solubility limit found in this study was $x = 0.15$, much higher than the reported value ($x = 0.04$) for bulk ceramic material. The metastable solubility limit of $x = 0.33$ for as-grown epitaxial films is also shown by the arrow denoted as the LMBE limit.

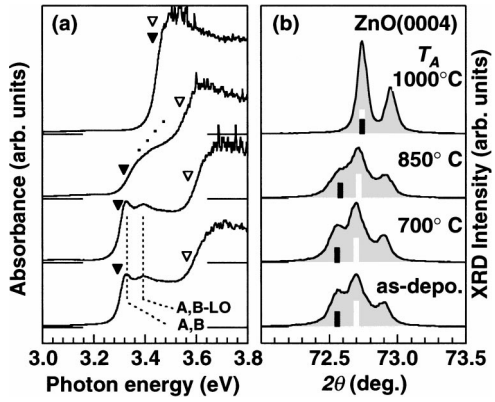


FIG. 3. Absorption spectra (a) and x-ray diffraction patterns (b) of a $Mg_{0.15}Zn_{0.85}O$/ZnO bilayer film annealed at various temperatures. Open and closed triangles in (a) show the band edges of $Mg_{0.15}Zn_{0.85}O$ and ZnO, respectively. White and black bars in (b) indicate the position and integrated intensity of the $K\alpha_1$ diffraction peak from the $Mg_{0.15}Zn_{0.85}O$ and ZnO layers, respectively. After 850 °C annealing, considerable broadening was observed in both the absorption spectrum and the XRD pattern, indicating Mg diffusion across the heterointerface. After 1000 °C annealing, diffusion was completed to form a $Mg_{0.08}Zn_{0.92}O$ alloy film.

3.56 eV. The $x = 0.22$ film showed a decrease of E_g after annealing at 850 °C, and finally, E_g was decreased to a value identical to that of the $x = 0.15$ film. Therefore, the segregation of RS precipitates left the saturated WZ $Mg_xZn_{1-x}O$ matrix with lower x. Here, we conclude the thermodynamic solubility limit of MgO in ZnO is $x = 0.15$ at 1000 °C.

Now, we examine the thermal stability of the $Mg_xZn_{1-x}O$/ZnO heterointerface with $x = 0.15$ (just at the solubility limit) and $x = 0.23$ (far above the solubility limit). The thickness of the $Mg_xZn_{1-x}O$ was 170 and 230 nm for the $x = 0.15$ and $x = 0.23$ films, respectively, and that of ZnO was 150 nm for both the films. Figure 3(a) shows the absorption spectra for the $x = 0.15$ bilayer. The spectra for films as-deposited and annealed at 700 °C showed clear absorption edges at 3.29 and 3.56 eV, corresponding to the band edge of ZnO and $Mg_{0.15}Zn_{0.85}O$ layers, respectively. *A*- and *B*-exciton- (*A*,*B*) and LO-phonon-assisted excitonic absorption (*A*,*B*−LO) (Ref. 15) peaks are also clearly seen as indicated by the dotted lines. After annealing at 850 °C, the absorption edge became broad. Upon annealing at 1000 °C, the absorption spectrum looks like that of the $x = 0.08$ film, showing a single band edge at 3.43 eV. The XRD patterns shown in Fig. 3(b) also clearly indicate similar Mg interdiffusion behavior. Below 850 °C, XRD patterns of a bilayer heteroepitaxial film having different *c*-axis lattice constants can be seen. After annealing at 1000 °C, the XRD pattern demonstrates a single component film. We summarize the E_g values for the two heteroepitaxial bilayers ($x = 0.15$ and $x = 0.23$) in Fig. 4. Below 700 °C, the bilayer structure is stable. For the bilayer having supersaturated ($x = 0.23$) $Mg_xZn_{1-x}O$, the thermal diffusion is completed after annealing at 850 °C. When thermodynamically stable $Mg_xZn_{1-x}O$ ($x = 0.15$) is combined with pure ZnO, a better thermal stability is demonstrated by the fact that thermal diffusion of Mg starts at 850 °C and is completed after the annealing at 1000 °C.

The stability of alloy films and heterostructures is summarized in Fig. 5. Below 700 °C, supersaturated films and heterointerfaces are stable. The thermal stability of these het-

Downloaded 27 Oct 2004 to 130.34.226.195. Redistribution subject to AIP license or copyright, see http://apl.aip.org/apl/copyright.jsp

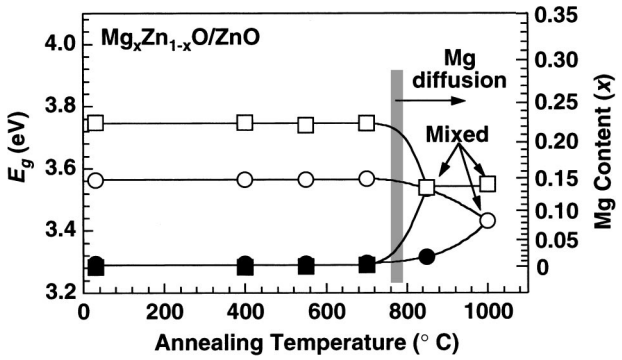


FIG. 4. Band gap (E_g) of $Mg_xZn_{1-x}O$ (open symbols) and ZnO layers (closed symbols) deduced from the absorption spectra in Fig. 3(a). ● and ○ are for the bilayer of $Mg_{0.15}Zn_{0.85}O$/ZnO, and ■ and □ are for the bilayer of $Mg_{0.23}Zn_{0.77}O$/ZnO. Mg diffusion occurred when annealing was done at temperatures above 850 °C for both samples. The $x=0.23$ sample showed complete alloying at a lower temperature than the $x=0.15$ sample. The vertical band denotes the temperature at which Mg diffusion initiates.

erointerfaces is much better than that of other II–VI semiconductors. For instance, a few minutes annealing in nitrogen ambient induced considerable interdiffusion in $ZnSe/ZnS_{0.16}Se_{0.84}$ (<650 °C) (Ref. 16) and $Zn_{0.79}Cd_{0.21}Se/ZnSe$ (<600 °C).[17] However, when supersaturated $Mg_xZn_{1-x}O$ with $x>0.15$ compositions are used in heteroepitaxial devices, considerable instability due to microscopic segregation has to be taken into account. In fact, when we made superlattices composed of ZnO and $Mg_xZn_{1-x}O$ with $x=0.10$ and 0.20 (Ref. 12), the former superlattice showed clear quantum size effects as seen in other III–V compound semiconductors, whereas the latter showed nonideal properties which can be attributed to the inhomogeneous Mg distribution in the $Mg_xZn_{1-x}O$ barrier

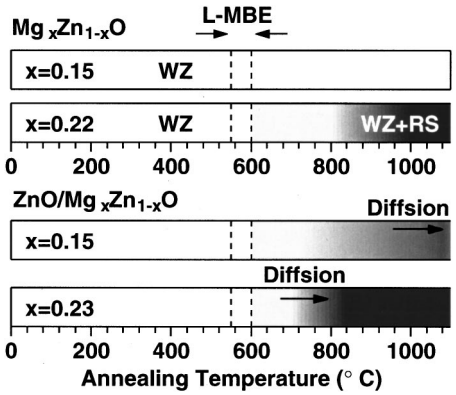


FIG. 5. The instability of supersaturated $Mg_xZn_{1-x}O$ alloy films and $Mg_xZn_{1-x}O$/ZnO heterointerfaces is summarized. The typical LMBE temperature range for epitaxial growth is much lower than the segregation threshold temperature (~800 °C) and diffusion threshold temperature (~700 °C).

layers. Therefore, although the present study indicates that the supersaturated $Mg_xZn_{1-x}O$ films can be stable below 700 °C, the microscopic distribution of Mg may have inhomogeneity when x exceeds 0.15.

In conclusion, we have examined the thermal stability of $Mg_xZn_{1-x}O$ alloy films and their heterostructures with pure ZnO. An apparent solubility limit was determined as $x=0.15$. Supersaturated alloy films with $x=0.22$ showed segregation of MgO starting around 850 °C and reaching steady state at 1000 °C. ZnO/$Mg_xZn_{1-x}O$ heterostructures were stable up to 700 °C. These temperatures give us enough margin for the fabrication of high-quality thin films and heterostructures based on ZnO, which have typical deposition temperatures around 550 °C.

This work was partly supported by JSPS Research for the Future Program in the area of Atomic-Scale Surface and Interface Dynamics (RFTF96P00205) and NEDO Proposal-based Research (99S12010). One of the authors (A.O.) is supported by JSPS Research Fellowships for Young Scientists.

[1] D. C. Reynolds, D. C. Look, and B. Jogai, Solid State Commun. **99**, 873 (1996).
[2] P. Yu, Z. K. Tang, G. K. L. Wong, M. Kawasaki, A. Ohtomo, H. Koinuma, and Y. Segawa, in *23rd International Conference on the Physics of Semiconductors*, edited by M. Scheffler and R. Zimmermann (World Scientific, Singapore, 1996), p. 1453.
[3] D. M. Bagnall, Y. F. Chen, Z. Zhu, T. Yao, S. Komiya, M. Y. Shen, and T. Goto, Appl. Phys. Lett. **70**, 2230 (1997).
[4] Y. Segawa, A. Ohtomo, M. Kawasaki, H. Koinuma, Z. K. Tang, P. Yu, and G. K. L. Wong, Phys. Status Solidi B **202**, 669 (1997).
[5] See, for example, a review, M. Kawasaki, A. Ohtomo, I. Ohkubo, H. Koinuma, Z. K. Tang, P. Yu, G. K. L. Wong, B. P. Zhang, and Y. Segawa, Mater. Sci. Eng., B **56**, 239 (1998).
[6] Z. K. Tang, G. K. L. Wong, P. Yu, M. Kawasaki, A. Ohtomo, H. Koinuma, and Y. Segawa, Appl. Phys. Lett. **72**, 3270 (1998).
[7] K. Minegishi, Y. Koiwai, Y. Kikuchi, K. Yano, M. Kasuga, and A. Shimizu, Jpn. J. Appl. Phys., Part 2 **36**, L1453 (1997).
[8] T. Yamamoto and H. Yoshida, Jpn. J. Appl. Phys., Part 2 **68**, L166 (1999).
[9] A. Ohtomo, M. Kawasaki, T. Koida, K. Masubuchi, H. Koinuma, Y. Sakurai, Y. Yoshida, T. Yasuda, and Y. Segawa, Appl. Phys. Lett. **72**, 2466 (1998).
[10] Y. Matsumoto, M. Murakami, Z. W. Jin, A. Ohtomo, M. Lippmaa, M. Kawasaki, and H. Koinuma, Jpn. J. Appl. Phys., Part 2 **38**, L603 (1999).
[11] M. Kawasaki, A. Ohtomo, R. Shiroki, I. Ohkubo, H. Kimura, G. Isoya, T. Yasuda, Y. Segawa, and H. Koinuma, *Extended Abstracts of International Conference on Solid State Devices and Materials, Hiroshima, Japan* (1998), p. 356.
[12] A. Ohtomo, M. Kawasaki, I. Ohkubo, H. Koinuma, T. Yasuda, and Y. Segawa, Appl. Phys. Lett. **75**, 980 (1999).
[13] J. F. Sarver, Fred L. Katnack, and F. A. Hummel, J. Electrochem. Soc. **106**, 960 (1959).
[14] E. R. Segnit and A. E. Holland, J. Am. Ceram. Soc. **78**, 409 (1965).
[15] W. Y. Liang and A. D. Yoffe, Phys. Rev. Lett. **20**, 59 (1968).
[16] G. Bacher, D. Tonnies, D. Eisert, A. Forchel, M. O. Moller, M. Korn, B. Jobst, D. Hommel, G. Landwehr, J. Sollner, and M. Heuken, J. Appl. Phys. **79**, 4368 (1996).
[17] R. C. Tu, Y. K. Su, Y. S. Huang, and S. T. Chou, J. Appl. Phys. **84**, 6017 (1998).

Downloaded 27 Oct 2004 to 130.34.226.195. Redistribution subject to AIP license or copyright, see http://apl.aip.org/apl/copyright.jsp